Journal for ImmunoTherapy of Cancer

Inactivation of interleukin-30 in colon cancer stem cells via CRISPR/Cas9 genome editing inhibits their oncogenicity and improves host survival

Luigi D'Antonio,[1,2] Cristiano Fieni ,[1,2] Stefania Livia Ciummo,[1,2] Simone Vespa,[1] Lavinia Lotti,[3] Carlo Sorrentino,[1,2] Emma Di Carlo [1,2]

To cite: D'Antonio L, Fieni C, Ciummo SL, *et al*. Inactivation of interleukin-30 in colon cancer stem cells via CRISPR/Cas9 genome editing inhibits their oncogenicity and improves host survival. *Journal for ImmunoTherapy of Cancer* 2023;**11**:e006056. doi:10.1136/jitc-2022-006056

► Additional supplemental material is published online only. To view, please visit the journal online (http://dx.doi.org/10.1136/jitc-2022-006056).

LD and CF are joint first authors.

CS and EDC are joint senior authors.

Accepted 27 February 2023

[1]Dipartimento di Medicina e Scienze dell'Invecchiamento, Università degli Studi "G. d'Annunzio" di Chieti-Pescara, Chieti, Italy
[2]Center for Advanced Studies and Technology (CAST), Università degli Studi "G. d'Annunzio" di Chieti-Pescara, Chieti, Italy
[3]Department of Experimental Medicine, University of Rome La Sapienza, Rome, Italy

Correspondence to
Professor Emma Di Carlo; edicarlo@unich.it

ABSTRACT

Background Progression of colorectal cancer (CRC), a leading cause of cancer-related death worldwide, is driven by colorectal cancer stem cells (CR-CSCs), which are regulated by endogenous and microenvironmental signals. Interleukin (IL)-30 has proven to be crucial for CSC viability and tumor progression. Whether it is involved in CRC tumorigenesis and impacts clinical behavior is unknown.

Methods IL30 production and functions, in stem and non-stem CRC cells, were determined by western blot, immunoelectron microscopy, flow cytometry, cell viability and sphere formation assays. CRISPR/Cas9-mediated deletion of the *IL30* gene, RNA-Seq and implantation of *IL30* gene transfected or deleted CR-CSCs in NSG mice allowed to investigate IL30's role in CRC oncogenesis. Bioinformatics and immunopathology of CRC samples highlighted the clinical implications.

Results We demonstrated that both CR-CSCs and CRC cells express membrane-anchored IL30 that regulates their self-renewal, via WNT5A and RAB33A, and/or proliferation and migration, primarily by upregulating CXCR4 *via* STAT3, which are suppressed by IL30 gene deletion, along with WNT and RAS pathways. Deletion of *IL30* gene downregulates the expression of proteases, such as MMP2 and MMP13, chemokine receptors, mostly CCR7, CCR3 and CXCR4, and growth and inflammatory mediators, including ANGPT2, CXCL10, EPO, IGF1 and EGF. These factors contribute to IL30-driven CR-CSC and CRC cell expansion, which is abrogated by their selective blockade. *IL30* gene deleted CR-CSCs displayed reduced tumorigenicity and gave rise to slow-growing and low metastatic tumors in 80% of mice, which survived much longer than controls. Bioinformatics and CIBERSORTx of the '*Colorectal Adenocarcinoma TCGA Nature 2012*' collection, and morphometric assessment of IL30 expression in clinical CRC samples revealed that the lack of IL30 in CRC and infiltrating leucocytes correlates with prolonged overall survival.

Conclusions IL30 is a new CRC driver, since its inactivation, which disables oncogenic pathways and multiple autocrine loops, inhibits CR-CSC tumorigenicity and metastatic ability. The development of CRISPR/Cas9-mediated targeting of IL30 could improve the current therapeutic landscape of CRC.

WHAT IS ALREADY KNOWN ON THIS TOPIC

⇒ Colorectal cancer (CRC) progression and related mortality are significant public health issue worldwide. Cancer stem cells (CSCs) drive tumor initiation and progression and Interleukin (IL)-30 has recently emerged as a key regulator of their behavior in both prostate and breast cancer. The involvement of IL30 in CRC oncogenesis and its clinical implications have never been investigated.

WHAT THIS STUDY ADDS

⇒ Both stem and differentiated CRC cells constitutively express IL30, which regulates their self-renewal and/or proliferation, migration and gene expression profile. Targeting of *IL30, via* CRISPR/Cas9 gene editing, suppresses, in both stem and non-stem CRC cells, oncogenic pathways and expression of inflammatory, growth, angiogenic and lymphangiogenic factors. Inactivation of IL30 inhibits colorectal CSC tumorigenicity and reduces tumor onset and progression, resulting in prolonged host survival. The lack of IL30 expression in clinical tumor samples is associated with an improved overall survival in CRC patients.

HOW THIS STUDY MIGHT AFFECT RESEARCH, PRACTICE OR POLICY

⇒ Strategies to restrain the CRC stem cell compartment may hinder tumor progression and recurrence and enhance response to current antitumor therapies. This study provides the proof of concept that selective targeting of IL30 inhibits CRC growth and metastasis and paves the way for the development of a new therapeutic tool for CRC patients.

INTRODUCTION

Colorectal cancer (CRC) is a leading cause of cancer-related death[1] and its mortality rate is expected to rise worldwide, due to population growth and aging, thus entailing a global public health challenge. CRC mortality is mainly due to therapy resistance and metastasis, which are driven by a small population

of cancer stem-like cells (CSCs), endowed with high tumorigenicity, self-renewal, multidirectional differentiation potential and abnormal activation of proliferative signaling, such as the WNT and RAS driven pathways.[2] In addition, CSCs can switch into a slow-proliferating or quiescent state, which has been associated with tumor progression,[3] and can be regulated by endogenous and environmental cues, including cytokines and growth factors.

The immunoregulatory cytokine, interleukin(IL)-30, has recently emerged as a novel regulator of CSC behavior, displaying autocrine and paracrine effects in the CSC niche microenvironments of both prostate and breast cancers.[4 5] Originally identified as the four α-helix bundle (cytokine-like) subunit (p28), which can bind Epstein-Barr virus Induced 3 (EBI3) to form the heterodimeric cytokine IL27,[6] IL30 can function as an autonomous cytokine with its own functional properties[7–9] that signals after binding to the IL6 Receptor subunit alpha (IL6Rα), or its soluble form (sIL6Rα), by recruiting a gp130 homodimer.[10] Targeting IL30 signaling in prostate and breast CSCs and host environment has proven to counteract tumor growth and to improve host survival.[5 11] The discovery of the CRISPR/Cas9 tool has revolutionized the field of genome editing, by providing high specificity, efficiency and versatility, and enabling the rapid development of effective in vivo targeted therapies for the treatment of different human diseases.[12]

This study provides evidence that IL30 is constitutively expressed in both stem and differentiated CRC cells, and that it supports their proliferation and/or self-renewal and migration abilities. Deletion of the *IL30* gene, in both cell types, by CRISPR/Cas9-mediated gene editing, reshapes their transcriptional profile by weakening the WNT and RAS pathways, turning off CRC-associated inflammation, angiogenesis and lymphangiogenesis, and by disabling an autocrine cascade of tumor growth and progression factors, which results in a significant inhibition of colorectal (CR)-CSC tumorigenicity and metastatic potential, that ultimately leads to prolonged host survival. Inactivation of IL30 signaling, by a safe and selective targeted approach, could improve the therapeutic scenario for patients with CRC.

MATERIALS AND METHODS

Cell cultures, MTT and sphere formation assays

CRC cells, HCT116, isolated from a poorly differentiated, high grade, CRC[13] and harboring an activating mutation of the KRAS (Merck, Darmstadt, Germany) were authenticated, using the STR analysis, by Eurofins Genomics (Ebersberg, Germany). Cells were confirmed mycoplasma-free, by PCR, and were cultured, for fewer than 6 months after resuscitation, in the medium recommended by the manufacturer.

CR-CSCs were derived from CRC cells and were authenticated, based on their expression of specific markers, by flow cytometry and by their growth properties in vitro, by sphere formation efficiency (using the Extreme Limiting Dilution Analysis), as described in the online supplemental materials and methods and, in vivo, by limiting dilution analysis, as described below.

Chemotaxis and migration assay

The migration of cancer cells toward CXCL12, was assessed with QCM 8 µm Chemotaxis Assay 24-well Colorimetric kit (Merck, Darmstadt, Germany), according to the manufacturer's instructions.

Flow cytometry

Cancer cells were stained with the antibodies (Abs) listed in the online supplemental table S1 and analyzed using a BD Scientific Canto II Flow Cytometer (RRID:SCR_018056). Dead cells were excluded by 7AAD staining and the data were analyzed using the FlowJo software (RRID:SCR_008520).

CRISPR/Cas9-mediated interleukin-30, WNT5A, RAB33A and STAT3 gene knockout

CRISPR/Cas9 gene editing was used to generate IL30KO-CRC cells and IL30KO-CR-CSCs cells, WNT5A-KO IL30-CR-CSCs, RAB33A-KO IL30-CR-CSCs, and STAT3-KO CR-CSCs, as described in the online supplemental materials and methods. Gene deletions were validated by Sanger sequencing and Western blotting (WB).

Transfection with IL30 expressing vector

Generation of the IL30 lentiviral expression vector and its transfection into CRC cells and CR-CSCs were performed as described in the online supplemental materials and methods. Expression of IL30 was confirmed by real-time RT-PCR and WB.

Real-time RT-PCR

RNA was extracted from cancer cells by using the RNeasy Mini Kit (#74104), and reverse-transcribed with the QuantiTect Rev. Transcription Kit (#205311) (Qiagen, Hilden, Germany). Analysis of *IL30* mRNA levels were performed as described in the online supplemental materials and methods.

Whole transcriptome sequencing

RNA extracted from cancer cells was frozen in liquid nitrogen and shipped to Macrogen Europe (Amsterdam, NL), which performed RNA-Seq by using the Illumina Platform (RRID:SCR_010233). Trimmed reads were mapped to a reference genome with HISAT2 (RRID:SCR_015530) and the expression profile was calculated for each transcript as read count, FPKM (Fragment per Kilobase of transcript per Million mapped reads) and TPM (Transcripts Per Kilobase Million). DEG (Differentially Expressed Genes) analysis was performed

using edgeR (RRID:SCR_012802) and the results were expressed as fold changes. A significant threshold of a twofold change in gene expression corresponded to a $p<0.05$.

Immunoelectron microscopy

Immunogold labeling of IL30 in CR-CSCs was performed as described in the online supplemental materials and methods and analyzed using Philips CM10 and Fei Philips Morgagni 268D transmission electron microscopes (Philips, Amsterdam, NL).

WB and ELISA

WB, to assess the production of IL30, WNT3A, WNT5A, MMP2, MMP13, RAB33A and STAT3, and ELISA, for the quantitation of ANGPT2, CXCL10, EPO, EGF, IGF1, IL6 and VEGFA, in both CRC cells and CR-CSCs, were carried out as described in the online supplemental materials and methods.

Mouse studies

NSG mice were purchased from Charles River (Wilmington, MA, USA) and were housed, according to the Jackson Laboratory's guidelines, in the animal facility of the Center for Advanced Studies and Technology, Chieti, Italy. All animal procedures were performed in accordance with the European Community and ARRIVE guidelines and were approved by the Institutional Animal Care Committee of 'G. d'Annunzio' University and by the Italian Ministry of Health (Authorization n. 399/2015 PR). The tumorigenicity of CR-CSCs was assessed by limiting dilution analysis, by subcutaneously (s.c.) injecting, in NSG (NOD *scid* gamma) mice, a range from 1×10^1 to 5×10^3 CR-CSCs per animal (20 mice per group).

To evaluate in vivo the effects of *IL30* gene overexpression or knockout (KO), three groups (90 animals, all siblings) of the thirty 8-week-old female NSG mice (NOD.Cg-Prkdc^{scid} Il2rg^{tm1Wjl}/SzJ) were s.c. injected with 3×10^3 wild type (WT), Empty Vector (EV) or human IL30 lentiviral-DNA-transfected (IL30-over) CR-CSCs, and another three groups (90 animals, all siblings) of thirty 8-week-old female NSG mice were s.c. injected with 5×10^3 WT, non-targeting guide RNA-treated (NTgRNA), or IL30KO CR-CSCs. Animals were housed as described in the online supplemental materials and methods. Based on tumor growth and progression rate, 15 mice from each group were euthanized at key time points (3 mice per point) for histopathological analyses. The remaining 15 mice per group were kept until tumors reached 3 cm^3 or evidence of suffering was observed. Autopsy and histopathological examinations of liver, lungs, kidney and spleen were performed. An overall sample size of 15 mice per group allowed the detection of a statistically significant difference, in tumor growth, between three groups, with an 80% power, at a 0.05 significance level (G*Power, RRID:SCR_013726).

Patients and samples

Normal and tumor tissue samples were obtained from 120 patients undergoing colectomy for CRC, between 2009 and 2016, at the 'SS Annunziata' Hospital of Chieti, Italy. CRC patients, ages 37–83, were followed-up for at least 5 years after the colectomy (table 1). The size of the patient cohort allowed the detection of a statistically significant difference between three groups, with an 82% power and a 5% significance level (G*Power, RRID:SCR_013726).

Immunopathology and morphometric analyses

Histology, immunohistochemistry (performed with the Abs listed in the online supplemental table S2), and assessment of proliferation index, microvessel and immune cell counts (in tumor xenografts), were performed as described in the online supplemental materials and methods.

For the morphometric analyses of IL30 expression, in CRC specimens, previously applied criteria[11] were used, and described in the online supplemental materials and methods. Based on morphometric analysis, CRC samples with positive and strong IL30 expression were classified as IL30$^{+/+}$, CRC samples with negative and scanty IL30 expression were classified as IL30$^{-/-}$, whereas the remaining CRC samples with different expression levels of IL30, ranging from weakly positive to negative in neoplastic epithelia, and from distinct to scanty in the immune cell infiltrate, were defined as IL30$^{+/-}$ CRCs.

Bioinformatic analyses

For bioinformatic analyses, RNA-Seq data of tumor samples from the '*CRC TCGA Nature 2012*' collection, which includes 276 CRC cases, were downloaded from the cBioportal for Cancer Genomics database (https://www.cbioportal.org; cBioPortal, RRID:SCR_014555).

For each CRC sample, the Z-score of the expression level for each gene of interest was calculated based on the mean and SD of all the samples in the study. In CRC samples of the '*TCGA Nature 2012*' collection, the expression of IL30 was never below a Z-score=-2, therefore CRC samples with a Z-score ≥2 were defined as high expressing tumors, whereas CRC samples with a Z-score <2 were defined as moderate expressing tumors.

Survival curves were constructed, with CRC cases for which both gene expression and follow-ups were available (online supplemental table S3), after the exclusion of cases that also overexpressed EBI3 or CRLF1, using the Kaplan-Meier method. Survival differences were analyzed by the log-rank test.

The association between IL30 gene expression and tumor size, disease stage, CRC molecular subtype and patients' sex and age was assessed using χ^2 and Cramér's V tests.

CIBERSORTx

To estimate the expression of IL30 in the immune cell subsets infiltrating CRC samples (online supplemental

Table 1 Clinical-pathological characteristics of patients with CRC* and immunohistochemical staining for IL30 in their tumor samples

			IL30 immunostaining			
	No of patients	Percentages	$IL30^{+/+}$	$IL30^{+/-}$	$IL30^{-/-}$	P value
Sex						
Female	56	46.32%	8 (14.39%)	42 (75.56%)	6 (10.79%)	0.823†
Male	64	53.68%	10 (15.52%)	45 (69.86%)	9 (13.97%)	0.823†
Total	120	100.00%	18 (15.00%)	87 (72.50%)	15 (12.50%)	
Age						
≤40	7	6.01%	1 (13.87%)	5 (69.33%)	1 (13.87%)	1‡
41–50	10	8.32%	1 (10.02%)	8 (80.13%)	1 (10.02%)	0.999‡
51–60	22	18.73%	4 (17.80%)	15 (66.74%)	3 (13.35%)	0.803‡
61–70	37	30.42%	5 (13.70%)	27 (73.96%)	5 (13.70%)	0.999†
71–80	33	27.31%	5 (15.26%)	24 (73.23%)	4 (12.21%)	0.999‡
≥81	11	9.21%	2 (18.10%)	8 (72.39%)	1 (9.05%)	0.881‡
Total	120	100.00%	18 (15.00%)	87 (72.50%)	15 (12.50%)	
Clinical stage						
Stage I	22	18.50%	3 (13.51%)	18 (81.08%)	1 (4.50%)	0.518‡
Stage II	45	37.19%	7 (15.69%)	30 (67.22%)	8 (17.93%)	0.375†
Stage III	35	29.22%	5 (14.26%)	26 (74.15%)	4 (11.41%)	0.999‡
Stage IV	18	15.09%	3 (16.57%)	13 (71.79%)	2 (11.04%)	1‡
Total	120	100.00%	18 (15.00%)	87 (72.50%)	15 (12.50%)	
Molecular subtype						
CMS1	19	16.20%	2 (10.29%)	15 (77.16%)	2 (10.29%)	0.921‡
CMS2	52	43.00%	8 (15.50%)	37 (71.71%)	7 (13.57%)	0.951†
CMS3	12	10.33%	2 (16.13%)	9 (72.60%)	1 (8.07%)	1‡
CMS4	24	20.03%	4 (16.64%)	16 (66.57%)	4 (16.64%)	0.708‡
Mixed	13	10.44%	2 (15.96%)	10 (79.82%)	1 (7.98%)	0.999‡
Total	120	100.00%	18 (15.00%)	87 (72.50%)	15 (12.50%)	

*CRC patients had not received immunosuppressive treatments, or radiotherapy, and were free from immune system diseases.
†P values calculated using χ^2 test.
‡P values calculated using Fisher's exact test.
CMS, consensus molecular subtypes; CRC, colorectal cancer.

table S3), TPM-normalized RNA-seq data of the '*CRC TCGA Nature 2012*' collection was downloaded from http://firebrowse.org and analyzed using CIBERSORTx (RRID:SCR_016955), as described in the online supplemental materials and methods.

Statistical analyses

Between group differences were assessed by Student's t-test, or analysis of variance (ANOVA), followed by Tukey HSD test. Association between IL30 immunostaining in CRC samples and patients' sex, age, TNM staging and molecular subtype were assessed by Chi-squared or Fisher's exact test (when, at least, one category had an expected frequency <5). Survival curves were constructed using the Kaplan-Meier method and survival differences were analyzed by the log-rank test. Experiments were performed, at least, in triplicate.

All statistical tests were evaluated at an α level of 0.05 using Stata V.13 (StataCorp).

RESULTS

Stem and non-stem CRC cells express Interleukin-30, which sustains their self-renewal and/or proliferation

To assess whether IL30 was implicated in colorectal tumorigenesis, we first isolated CR-CSCs from a well characterized CRC line, HCT116,[13] and investigated the expression and response to IL30 in both stem and differentiated CRC cells.

While CRC cells grew in adhesion (figure 1A), CR-CSCs formed 3D spheroids (figure 1B) and revealed endless self-renewal ability and tumorigenicity at very low cell number, as demonstrated by limiting dilution experiments (figure 1C). To exclude differentiated cells, CR-CSCs were phenotypically validated, by flow cytometry, as $CD24^{+}CD26^{+}CD44v6^{+}CD133^{+}CD166^{+}ALDH1^{high}$-$EpCAM^{high}$cells (figure 1D).

Because of its amino acid sequence and tertiary structure, which is predictive of a single-pass type I

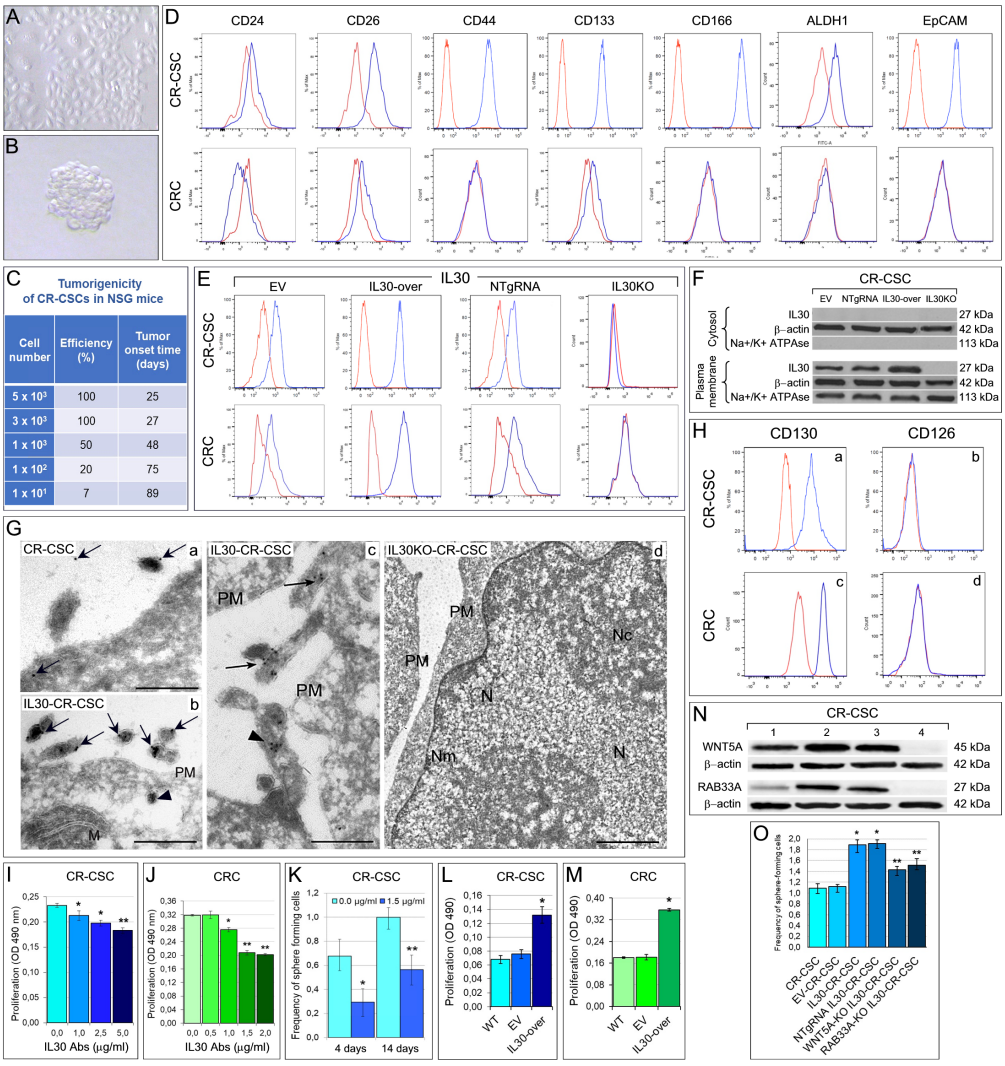

Figure 1 Expression of IL30 in CRC cells and CR-CSCs and IL30 dependent regulation of their viability. (A, B) Growth in adherence of CRC cells (A) and in suspension of CR-CSCs (B). (C) In vivo limiting dilution assay of CR-CSCs subcutaneously implanted in NSG mice. (D) Cytofluorimetric analyses of stem cell markers in CR-CSCs (top pictures), and in CRC cells (bottom pictures). Blue lines: specific Abs. Red lines: isotype controls. (E) Cytofluorimetric analyses of IL30 expression in CR-CSCs (top pictures) and CRC cells (bottom pictures). Red lines: isotype control. Blue lines: anti-IL30 Abs. Results obtained from WT cells were comparable with those from EV-transfected and NTgRNA-treated cells. (F) WB of IL30 protein expression in the cytosolic and plasma membrane fractions of EV-transfected and IL30-gene-transfected, NTgRNA-treated and IL30KO CR-CSCs. Results obtained from WT cells were comparable with those from EV-transfected and NTgRNA-treated cells. (G) Cryo-immunoelectron-microscopy showing IL30 localization, by gold particles, in WT (a), IL30 overexpressing (b, c) and IL30KO (d) CR-CSCs. The gold particles were frequent in IL30-CR-CSCs (b, c) compared with CR-CSCs (a) and absent in IL30KO-CR-CSCs (d). Gold particles mainly localized in the cytoplasmic membranes, along microvilli-like protrusions (arrows) or in the plasma membrane invaginations (arrowheads). PM, plasma membrane; N, nucleus; Nc, nucleolus; Nm, nuclear membrane; M, mitochondrion. Scale bars: 100 nm. (H) Cytofluorimetric analyses of gp130 (CD130) and IL6Rα (CD126) expression in CR-CSCs (a, b) and CRC cells (c, d). Red lines: isotype control. (I, J) MTT assay of CR-CSCs (I) and CRC cells (J), after 48 hours of treatment with anti-IL30 Abs. ANOVA: p<0.0001. *p<0.01, Tukey HSD test compared with 0.0 μg/mL (I) or 0.0 and 0.5 μg/mL (J). **p<0.05, Tukey HSD test compared with 0.0, 1.0 and 2.5 μg/mL (I) or 0.0, 0.5 and 1.0 μg/mL (J). (K) Sphere forming assay, evaluated by ELDA, of CR-CSCs, after 4 and 14 days of treatment with anti-IL30 Abs (1.5 μg/mL). *p<0.0001, $\chi 2$ test compared with untreated cells. **p=0.001, $\chi 2$ test compared with untreated cells. These results are comparable to those obtained from the sphere forming assay of IL30KO-CR-CSC cells versus untreated wild type and NTgRNA cells. (L, M) MTT assay of IL30-CR-CSCs (L) and IL30-CRC cells (M) cells, versus EV transfected and WT cells. (L, M) ANOVA, p<0.0001. *p<0.01, Tukey HSD test compared with EV transfected and WT cells. (N) WB analyses of WNT5A and RAB33A protein expression in CR-CSCs (Lane 1), IL30-CR-CSCs (Lane 2), NTgRNA-treated IL30-CR-CSCs (Lane 3) and WNT5A (top pictures) or RAB33A (bottom pictures) gene-deleted IL30-CR-CSCs (Lane 4). Results obtained from EV-CR-CSCs were comparable with those from CR-CSCs. (O) Sphere forming assay, evaluated by ELDA, of CR-CSCs, IL30-CR-CSCs and WNT5A or RAB33A gene deleted IL30-CR-CSCs. *p<0.0001, $\chi 2$ test compared with CR-CSCs and EV-CR-CSCs. **p<0.001, $\chi 2$ test compared with CR-CSCs, EV-CR-CSCs and IL30-CR-CSCs treated or untreated with NTgRNA. ANOVA, analysis of variance; CRC, colorectal cancer; CR-CSCs, colorectal cancer stem cells; ELDA, Extreme Limiting Dilution Analysis; EV, empty vector; WT, wild type.

transmembrane helix,[5 14] human IL30 is not released, unless it heterodimerizes with soluble receptor-like proteins, EBI3 or cytokine receptor-like factor 1 (CRLF1). Therefore, we looked for its expression in the plasma membrane of both stem and non-stem CRC cells. Both cell types expressed membrane-bound IL30, as shown by flow cytometry (figure 1E) and confirmed by WB, which discriminated the plasma membrane proteins from the cytoplasmic protein fractions (figure 1F). Cryo-immunoelectron microscopy, performed to visualize IL30 expression at the subcellular level, showed immunogold labeling in the plasma membrane and endoplasmic reticulum of CR-CSCs (figure 1G,a–d).

To assess whether membrane-bound IL30 can affect, via juxtacrine signaling, neighboring cells, we analyzed their expression of IL30 receptor chains, and determined their viability, both after CRISPR/Cas9-mediated knockout of *IL30* (IL30KO-CR-CSC) or by adding neutralizing anti-IL30 Abs, and following IL30 overexpression, by gene transfection (IL30-CR-CSC).

Although both stem and differentiated CRC cells lacked the IL6Rα (CD126) chain, and only expressed gp130 (CD130) (figure 1H), knockout of the IL30 gene or selective blockade of constitutively produced IL30, with anti-IL30 Abs, substantially inhibited proliferation (ANOVA: $p<0.0001$) in both cell types and self-renewal (χ^2 test: $p<0.005$) of CR-CSCs (figure 1I–K), which were significantly (ANOVA: $p<0.0001$; χ^2 test: $p<0.01$) increased by the forced overproduction of IL30, (figure 1L,M and online supplemental figure S1). Conversely, no effect on apoptosis was seen, in both stem and non-stem CRC cells following IL30 overexpression (online supplemental figure S2). Despite the absence of membrane-bound IL6α receptor (IL6R), the availability of soluble (s)IL6R (10.71±2.24 pg/mL in the supernatant of CR-CSCs, and 25.38±2.22 pg/mL in the supernatant of CRC cells), allows the formation of a biologically active complex, IL30/sIL6R, and subsequent trans-signaling through the recruitment of two gp130 chains.[10]

As expected, the addition of anti-sIL6R Abs to the culture medium of IL30-CR-CSCs, significantly inhibited their hyperproliferation, and suppressed WT and EV-CR-CSC proliferation (online supplemental figure S3A). Similar results were obtained with CRC cells (online supplemental figure S3B).

Since IL6 can compete with IL30 for binding with sIL6R,[7 10] we assessed its implication in IL30 activity, and therefore we analyzed whether CR-CSCs were able to produce IL6, or if this cytokine could be induced by IL30 and mediate its proliferative effect. CR-CSCs constitutively released 11.82±0.68 pg/mL of IL6, and CRC cells released 18.02±2.12 pg/mL of IL6, however, the blockade of this cytokine, with different concentrations of neutralizing anti-IL6 Abs, left substantially unaltered their proliferation as well as IL30-CR-CSC and IL30-CRC cell hyperproliferation (online supplemental figure S3C). Moreover, the inhibition of proliferation due to the blockade of IL30, was unaffected by the addition of anti-IL6 Abs, and was comparable to that obtained with anti-sIL6R Abs (online supplemental figure S3D). In line with this finding, the level of IL6 secreted by IL30-CR-CSCs, and by IL30-CRC cells, was the same as that released by control cells, thus excluding its involvement in the IL30 dependent CRC and CR-CSC cell proliferation.

These data demonstrate the expression of a bioactive membrane-bound IL30 in stem and non-stem CRC cells and its potential to affect the viability of cancer cells lacking transmembrane IL6Rα, but secreting its soluble form.

Interleukin-30 gene deletion reprograms the transcriptional profile of stem and non-stem CRC cells

Since IL30 overexpression increased self-renewal and/or proliferation, in CR-CSCs and CRC cells, which were suppressed by IL30 knockout, we investigated, by using RNA-Seq, whether CRISPR/Cas9-mediated IL30 gene deletion could affect their gene signature (figure 2A–D and online supplemental table S4).

Abrogation of endogenous IL30 consistently inhibited, although to a different extent between the two cell lines, the expression of Zinc Finger Proteins (ZNFs), especially *ZNF20*, *ZNF541*, *ZNF429*, *ZNF157*, *ZNF781*, Extracellular Matrix Proteins, such as *COL24A1*, *COL5A3*, *COL9A1*, *MUC 8*, *MUC15*, *MUC6*, and Proteases, such as *ADAM 20*, *ADAM 33*, *ADAM 7*, *MMP21*, *MMP2* and *MMP13*, which was confirmed by WB (figure 2A,E). Expression of Protease Inhibitors, such as *SERPINA5A* and *SERPINI2*, which are involved in cell migration, angiogenesis, inflammation, and programmed cell death,[15 16] was also substantially downregulated (figure 2B,D).

IL30 deletion dramatically suppressed, in both CRC cells and CR-CSCs, the expression of TNF Superfamily Members, such as *LTB*, *TNF* and, particularly, *TNFSF10/TRAIL*, which may favor tumor immune evasion.[17] Also, WNT and RAS Family Members, such as *WNT8B*, *WNT3A*, *RAB3C* and, especially, *WNT5A* (figure 2A,E) and *RAB33A*, which have proven to be essential for the maintenance of stemness,[18 19] were heavily downregulated by IL30 deletion. Indeed, knockout of WNT5A or RAB33A genes substantially reversed the sphere formation efficiency of IL30-CR-CSCs versus control cells (figure 1N,O), strongly suggesting their involvement in the IL30-dependent self-renewal of CR-CSCs.

Expression of CRC Driver Genes, in particular *TRIB1-2-3*, *AKT1-3*, *CRIPTO1*, *APC2*, *ALK* and *JAK1*, along with that of Cell Cycle Regulators, such as *MYC* and *CCND2*, were dramatically suppressed, in both stem and differentiated CRC cells, whereas *RARB*, which function as a tumor suppressor in CRC,[20] was strongly upregulated (figure 2A–D).

Membrane proteins, such as *PROM2*, a pentaspan protein associated with plasma membrane protrusions,[21] and *LYVE1*, usually expressed in lymphatic endothelium,[21] were substantially suppressed by IL30 deletion, in CRC

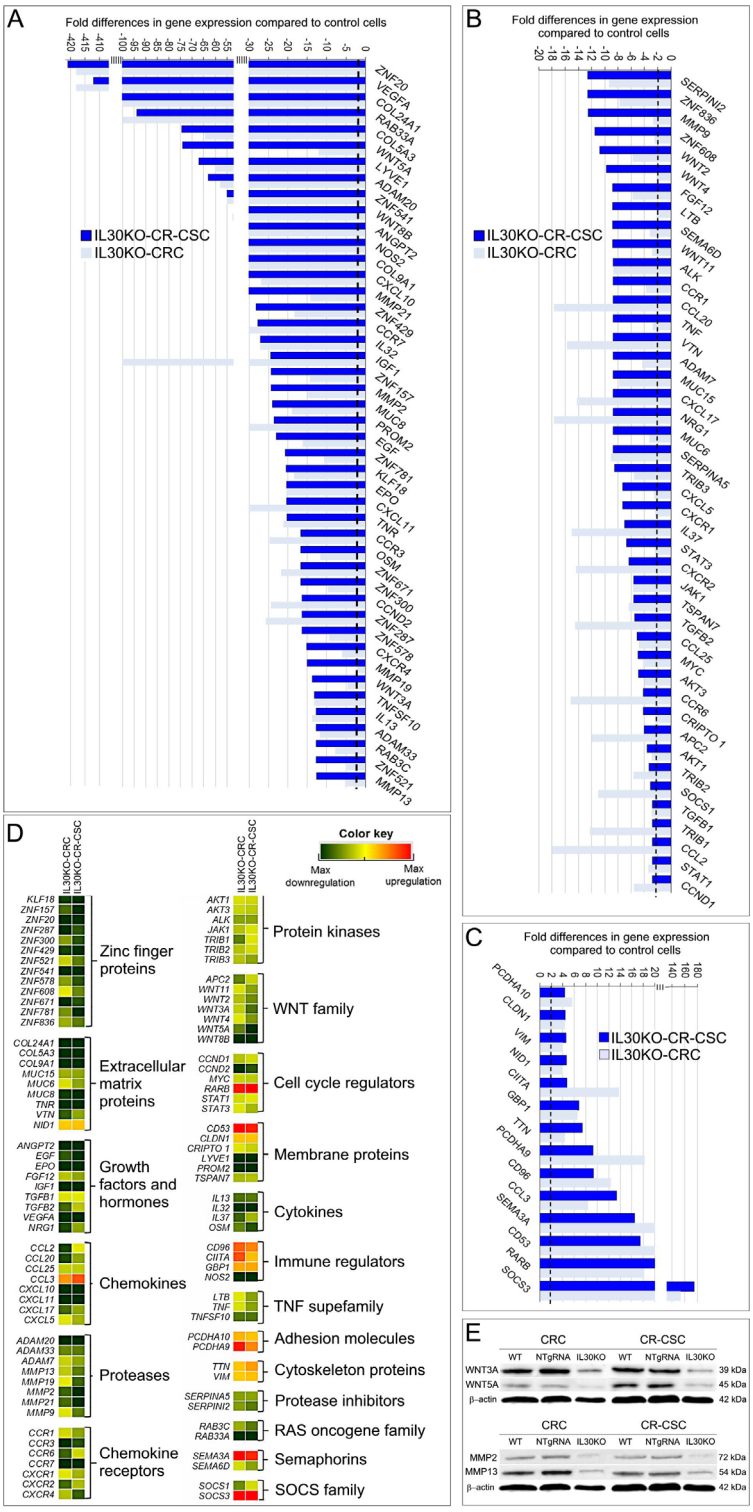

Figure 2 Regulation of the transcriptional profile of CRC cells and CR-CSCs by CRISPR/Cas9-mediated IL30 gene deletion. (A–C) Transcriptional profiling of IL30 gene deleted CRC cells and CR-CSCs showing the fold differences of the mRNAs of the downregulated (A, B) or upregulated (C) genes between IL30KO-CRC cells (light blue bars), or IL30KO-CR-CSCs (blue bars) and the respective NTgRNA-treated cells. Results obtained from untreated WT cells were comparable to those from control NTgRNA-treated cells. (A) Fold downregulation range from −421 to −13. (B) Fold downregulation range from −12.99 to 0. A significant threshold of a 2-fold change (dashed lines) in gene expression corresponded to p<0.001. (D) Heatmap illustrating RNA-Seq data of IL30KO-CRC cells and IL30KO-CR-CSCs versus the respective NTgRNA-treated cells. Differentially expressed genes are represented with a color scale ranging from green (maximum downregulation) to red (maximum upregulation). (E) WB analyses of WNT3A, WNT5A, MMP2 and MMP13 protein expression in IL30KO-CRC cells and IL30KO-CR-CSCs, and the respective WT and NTgRNA-treated cells. CRC, colorectal cancer; CR-CSC, colorectal cancer stem cell; WB, Western blotting; WT, wild type.

cells and CR-CSCs. By contrast, *CLDN1*, which regulates cell polarity and signal transductions, and the tetraspanin *CD53*, usually restricted to the immune compartment, were upregulated by IL30 deletion, in both CRC cells and CR-CSCs, along with genes coding for Adhesion Molecules, such as *PCDHA9* and *PCDHA10*, which may act as tumor and metastasis suppressors,[22] and Cytoskeleton Components, such as *TTN* and *VIM*.

The Semaphorin Family Members, *SEMA3A*, which inhibits angiogenesis,[23] but also T cell functions[24] and *SEMA6D*, which promotes tumor angiogenesis[25] were respectively upregulated and downregulated by IL30 deletion in both CRC cells and CR-CSCs (figure 2A–D).

SOCS family of proteins, which are classic negative feedback regulators of the JAK-STAT signaling pathway, were also regulated by IL30, since its deletion increased the expression of the tumor suppressor *SOCS3*,[26] and suppressed that of *SOCS1*, which may function as an oncogene in CRC.[27]

CRC cell expression of Immunoregulatory Molecules was also affected by IL30 gene knockout. Indeed, IL30 deletion upregulated *CD96*, usually expressed on T and NK cells, that when expressed in cancer may favor immune cell infiltration,[28] *CIITA*, which may drive MHCII expression, and *GBP1*, which acts as a tumor suppressor in CRC.[29] By contrast, IL30 deletion substantially downregulated *NOS2*, which plays a driving role in CRC (figure 2A–D).[30]

IL30 deletion also inhibited, in both CRC cells and CR-CSCs, the expression of Growth Factors and Hormones, primarily *ANGPT2, EGF, EPO, TGFβ1/2, IGF1* and *VEGFA*, immunosuppressive cytokines, such as *IL32, OSM, IL13* and *IL37*, Chemokines, including *CXCL10, CXCL11*, CXCL17, *CCL20* and CCL2, and chemokine receptors, including *CCR1/3/6/7, CCR3, CXCR1/2* and *CXCR4*, which can support cancer cell migration and metastatic dissemination.[31]

Interleukin-30 gene deletion suppresses CXCR4 expression in stem and non-stem CRC cells and reduces their migration toward CXCL12

Among the chemokine receptors, CXCR4 was the most to be downregulated in CRC cells and, primarily in CR-CSCs by CRISPR/Cas9-mediated IL30 deletion. Expression of CXCR4 by CR-CSCs promotes metastatic dissemination and confers poor patient prognosis.[31 32] CXCR4 overexpressing cells have demonstrated metastasis initiating capacity in CRC,[32] whereas targeting of $CXCR4^{+}$CR-CSCs reduces lung metastases,[33] therefore, supporting the metastasis initiating capacity of these cells. Here, we observed that expression of CXCR4 by CRC cells and CR-CSCs, which was improved by IL30 overexpression and reduced by IL30 knockout (figure 3A,B), promoted their migration in response to CXCL12 stimulation (figure 3C). This migration was prevented by neutralizing anti-CXCR4 Abs, and by anti-IL30 Abs, or IL30KO, of CRC cells and CR-CSCs, which has shown to suppress CXCR4 expression (figure 3C), therefore, suggesting the efficacy of targeting the IL30 gene in countering a pivotal mechanism of stem and non-stem CRC cell migration and metastasis. Notably, the IL30-dependent upregulation of CXCR4 in CR-CSCs and CRC cells, was substantially impaired by the deletion of the STAT3 gene (figure 3A,B and online supplemental figure S4), which our previous studies had suggested as the major mediator of IL30-dependent regulation of chemokine receptor expression.[4]

ANGPT2, CXCL10, EPO, IGF1 and EGF autocrine loops contribute to Interleukin-30 dependent proliferation and expansion of stem and non-stem CRC cells

In the wide range of genes coding for growth factors and inflammatory mediators regulated by IL30 in CR-CSCs and CRC cells, those coding for ANGPT2, CXCL10, EPO, IGF1, EGF and VEGFA were the most to be suppressed because of IL30 gene deletion. Therefore, we wondered if they were implicated in IL30-driven proliferation of stem and non-stem CRC cells.

Although at different levels, both cell types spontaneously produced and released ANGPT2, CXCL10, EPO, IGF1, EGF and, especially, VEGFA (online supplemental figure S5A–F) and, except for VEGFR1 and VEGFR2, they also expressed their cognate receptors, namely TIE2, CXCR3, EPOR, IGF1R and EGFR, (figure 4A). The production of these factors was consistently suppressed by the treatment with anti-IL30 Abs, or IL30KO, which substantiated RNA-Seq data. By contrast, it was significantly increased by IL30 overexpression, as demonstrated by ELISA (online supplemental figure S5A–F).

Neutralization of ANGPT2, CXCL10, EPO, IGF1 and EGF with specific Abs, inhibited both stem and non-stem CRC cell (CTRL) proliferation (ANOVA: $p<0.01$) (online supplemental figure S6A–E), which was significantly increased by the treatment with the respective recombinant proteins (ANOVA: $p<0.01$) (online supplemental figure S6F–J), that highlight their autocrine growth stimulating function.

Importantly, the increased proliferation of IL30 overexpressing stem and differentiated CRC cells versus CTRL cells, was substantially suppressed by the treatment with neutralizing Abs against each of the above described mediators (figure 4B–F), highly suggesting the cooperation of all of them in mediating IL30-driven proliferative boost.

CRISPR/Cas9-mediated deletion of Interleukin-30 in CR-CSCs prevents or delays tumor onset, reduces lung metastases and prolongs survival

To evaluate the effects of IL30 on CRC development both IL30-CR-CSCs and IL30KO-CR-CSCs were s.c. injected in NSG mice.

Twenty-six days after their implantation, IL30-CR-CSCs and control cells, WT-CR-CSCs and EV-CR-CSCs (figure 1C), gave rise to tumors that reached, on the 54th day, a mean volume (MTV) significantly higher in IL30 overexpressing than in control tumors

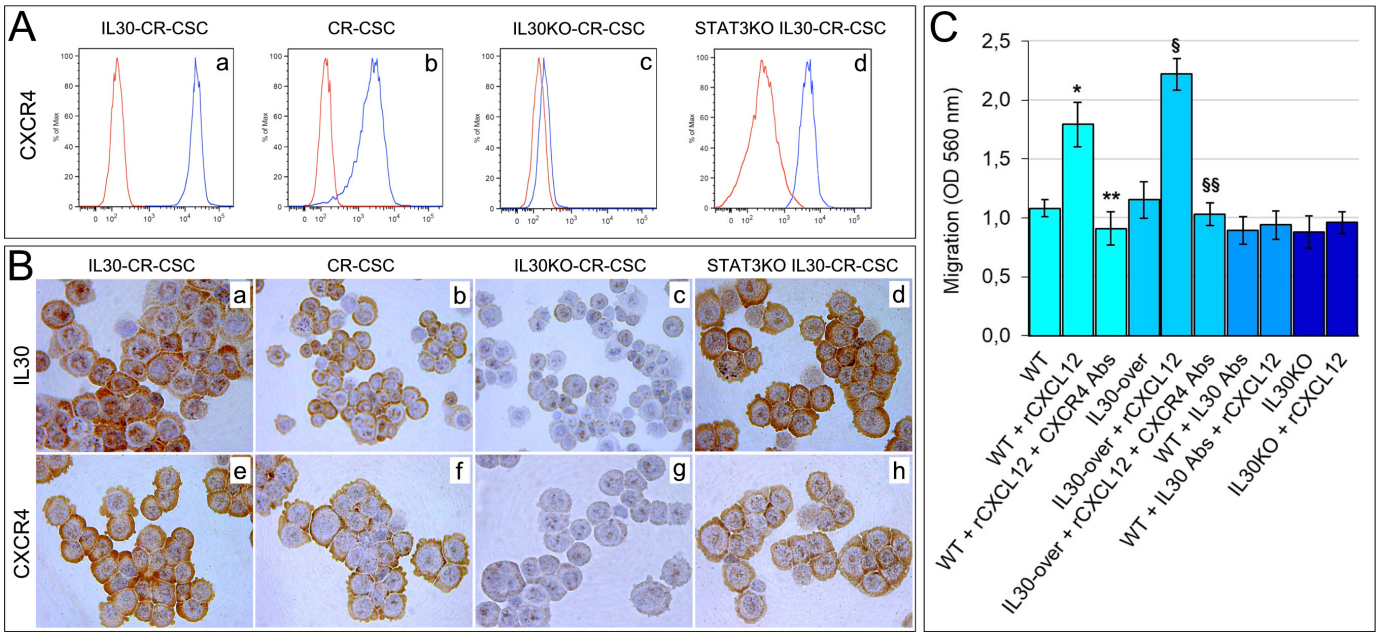

Figure 3 IL30-dependent regulation of CXCR4 expression impacts migration of CR-CSCs towards SDF1/CXCL12 ligand. (A) Cytofluorimetric analyses of CXCR4 expression in IL30-CR-CSCs (a), WT CR-CSCs (b), IL30KO-CR-CSCs (c) and STAT3KO IL30-CR-CSCs (d). Red lines: isotype control. Blue lines: anti-CXCR4 Abs. Results obtained from WT cells were comparable with those from EV-transfected and NTgRNA-treated cells. These results are comparable to those obtained from cytofluorimetric analyses of CXCR4 expression in CRC cells. (B) Immunocytochemical staining showing the expression of IL30 (a, b, c, d) and CXCR4 (e, f, g, h) in IL30-CR-CSCs, WT CR-CSCs, IL30KO-CR-CSCs and STAT3KO IL30-CR-CSCs. Magnification: X1000. These results are comparable to those obtained from immunocytochemical staining of CXCR4 expression in CRC cells. (C) Migration assay of WT (untreated or treated with anti-IL30 Abs), IL30 overexpressing and IL30KO CR-CSCs, with or without recombinant (r) CXCL12, as a chemoattractant, treated or not with anti-CXCR4 Abs. ANOVA, p<0.0001. *p<0.01, Tukey HSD test versus WT. **p<0.01, Tukey's HSD test versus WT+rCXCL12. §p<0.01, Tukey HSD test versus IL30-over and WT+rCXCL12. §§p<0.01, Tukey's HSD test versus IL30-over+rCXCL12. Results obtained from EV-transfected and NTgRNA-treated cells were comparable with those from WT cells. These results are comparable to those obtained from migration assay of CRC cells toward CXCL12. ANOVA, analysis of variance; CRC, colorectal cancer; CR-CSC, colorectal cancer stem cell; EV, empty vector; WT, wild type.

(MTV: IL30-CR-CSC, 3.073±0.495 cm^3 vs EV-CR-CSC, 1.663±0.176 cm^3 and vs CR-CSC, 1.677±0.180 cm^3. ANOVA, p<0.0001; *p<0.01 Tukey HSD test vs both CR-CSCs and EV-CR-CSCs) (figure 5A). By contrast, s.c. implantation, in NSG mice, of IL30KO-CR-CSCs, gave rise to tumors 81 days later, with a significant delay (56 days) compared with the control tumors (which arise 25 days after CSC implantation) (Fisher's exact test, p<0.0001), and only in 80% (12/15) of mice (Fisher's exact test, p<0.05) (figure 5B).

At the end of the experiment, autopsy and histopathological examination revealed that liver, kidney and spleen were metastasis-free (online supplemental figure S7), while the lungs were involved in tumor progression. Only 40% of mice bearing IL30KO tumors had developed lung metastasis vs 100% of control tumor-bearing mice (Fisher's exact test, p=0.0004 vs NTgRNA-CR-CSC or WT tumors. figure 5C). Furthermore, the average number of metastases per mouse was significantly lower in mice bearing IL30KO tumors than in mice bearing control tumors (0.4±0.52 in IL30KO tumors, vs 9.70±4.42 and 8.80±2.86 in WT and NTgRNA tumors, respectively. ANOVA, p<0.0001; Tukey HSD test, p<0.01 vs both controls. figure 5D,E) and did not correlate with the volume of the primary tumor (Pearson correlation coefficient: r=0.24). The slow-growing and low-metastatic IL30KO tumors resulted in a prolonged host survival (123 days vs 56 days of control groups) (log-rank test: p<0.0001), as shown by Kaplan-Meier curves (figure 5F).

Immunopathological analyses showed that IL30 overexpressing tumors were highly proliferating (Ki67: 84.29%±3.04%) and well vascularized (MVD: 12.13±2.10), when compared with WT and EV-transfected tumors (Ki67: 65.71±5.12%, and 69.00±3.32%, respectively. MVD: 5.43±2.07 and 5.57±1.81, respectively) (ANOVA, p<0.0001; Tukey HSD test, p<0.01 vs WT and EV tumors). By contrast, wide areas of ischemic-hemorrhagic necrosis characterized IL30 deficient tumors, which were low proliferating and poorly vascularized (Ki67: 27.38%±5.00%; MVD: 1.10±0.68) compared with WT (Ki67: 65.71%±5.12%; MVD: 5.43±2.07) and NTgRNA-CR-CSC tumors (Ki67: 70.29±5.38; MVD: 5.29±1.60) (ANOVA, p<0.0001; Tukey HSD test, p<0.01 vs WT and NTgRNA-CR-CSC tumors. figure 5G).

IL30-deficient tumors also lacked macrophage and granulocyte infiltrate that characterized IL30 overexpressing tumors (figure 5H,I), and lost the expression of inflammatory mediators, such as TNFα and CXCL5/

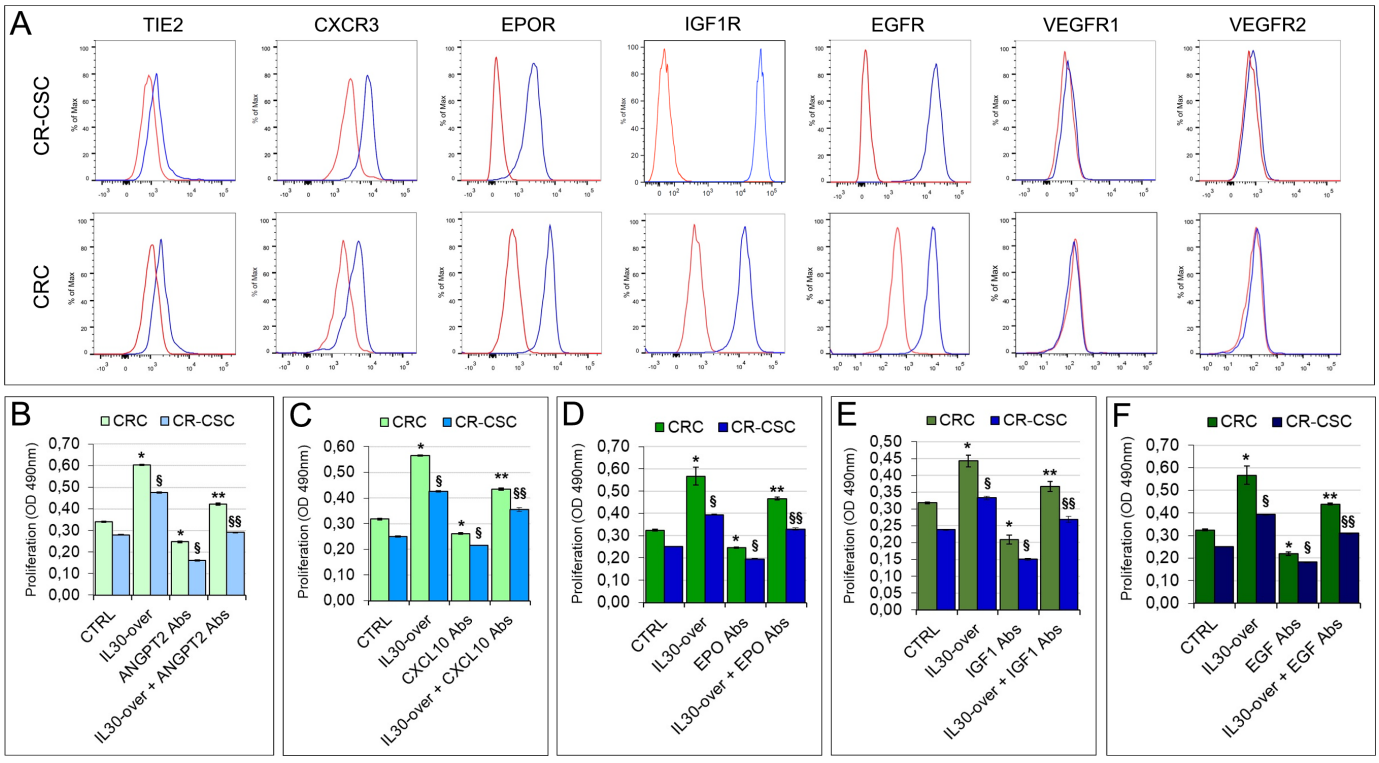

Figure 4 IL30-dependent regulation of growth factor and cytokine production in CRC cells and CR-CSCs, and IL30-driven autocrine growth loops. (A) Cytofluorimetric analyses of TIE2, CXCR3, EPOR, IGF1R, EGFR, VEGFR1 and VEGFR2 expression in CR-CSCs (top pictures) and CRC cells (bottom pictures). Red lines: isotype control. Blue lines: anti-TIE2, anti-CXCR3, anti-EPOR, anti-IGF1R, anti-EGFR, anti-VEGFR1 and anti-VEGFR2 Abs. (B) MTT assay of CRC cells and CR-CSCs (CTRL) and IL30-CRC cells and IL30-CR-CSCs (IL30-over), untreated or treated with anti-ANGPT2 Abs (2 µg/mL). ANOVA: p<0.0001. *,§p<0.01, Tukey's HSD test compared with CTRL cells. **,§§p<0.01, Tukey's HSD test compared with CTRL and IL30-CRC cells or IL30-CR-CSCs. Results obtained from EV transfected cells were comparable with those from CTRL cells. (C) MTT assay of CRC cells and CR-CSCs (CTRL) and IL30-CRC cells and IL30-CR-CSCs (IL30-over), untreated or treated with anti-CXCL10 Abs (2 µg/mL). ANOVA: p<0.0001. *,§p<0.01, Tukey HSD test compared with CTRL cells. **,§§p<0.01, Tukey HSD test compared with CTRL and IL30-CRC cells or IL30-CR-CSCs. Results obtained from EV-transfected cells were comparable with those from CTRL cells. (D) MTT assay of CRC cells and CR-CSCs (CTRL) and IL30-CRC cells and IL30-CR-CSCs (IL30-over), untreated or treated with anti-EPO Abs (0.5 µg/mL). ANOVA: p<0.0001. *,§p<0.01, Tukey HSD test compared with CTRL cells. **,§§p<0.01, Tukey HSD test compared with CTRL and IL30-CRC cells or IL30-CR-CSCs. Results obtained from EV transfected cells were comparable with those from CTRL cells. (E) MTT assay of CRC cells and CR-CSCs (CTRL) and IL30-CRC cells and IL30-CR-CSCs (IL30-over), untreated or treated with anti-IGF1 Abs (0.4 µg/mL). ANOVA: p<0.0001. *,§p<0.01, Tukey HSD test compared with CTRL cells. **,§§p<0.01, Tukey HSD test compared with CTRL and IL30-CRC cells or IL30-CR-CSCs. Results obtained from EV transfected cells were comparable with those from CTRL cells. (F) MTT assay of CRC cells and CR-CSCs (CTRL) and IL30-CRC cells and IL30-CR-CSCs (IL30-over), untreated or treated with anti-EGF Abs (2 µg/mL). ANOVA: p<0.0001. *,§p<0.01, Tukey HSD test compared with CTRL cells. **,§§p<0.01, Tukey HSD test compared with CTRL and IL30-CRC cells or IL30-CR-CSCs. Results obtained from EV transfected cells were comparable with those from CTRL cells. ANOVA, analysis of variance; CRC, colorectal cancer; CR-CSC, colorectal cancer stem cell; EV, empty vector.

ENA-78 (figure 5J), which may contribute to myeloid-derived cell recruitment, and growth factors, such as IGF1 and EGF, which contribute to IL30-driven CR-CSC and CRC cell proliferation (figure 5J). Tumors lacking IL30 also showed a reduced expression of LYVE1,[21] outlining both lymphatic vessels and spindle-shaped tumor cells (figure 5J), which enable lymphatic mimicry,[33] and reduction of VEGFA (figure 5K), which is involved in angiogenic switch and is associated with lymphatic metastases in CRC.[34] Expression of TGFβ1, STAT3 and JAK1, which are critically involved in tumorigenesis, were also dramatically downregulated in IL30KO tumors. By contrast, the tumor suppressor RARB, typically repressed *via* promoter methylation in CRC,[20] was considerably upregulated (figure 5K), thus substantiating, in vivo, the findings provided by RNA-Seq of IL30KO-CR-CSCs.

The lack of interleukin-30 expression in CRC and infiltrating leucocytes correlates with prolonged overall survival of CRC patients

The effects of IL30 deletion on the onset and progression of CSC-induced tumor xenograft, and its impact on the lifespan of tumor-bearing mice, led us to assess whether these findings may have translational implications. Therefore, we investigated IL30 expression in tumor samples from 120 patients, who underwent colectomy for CRC,

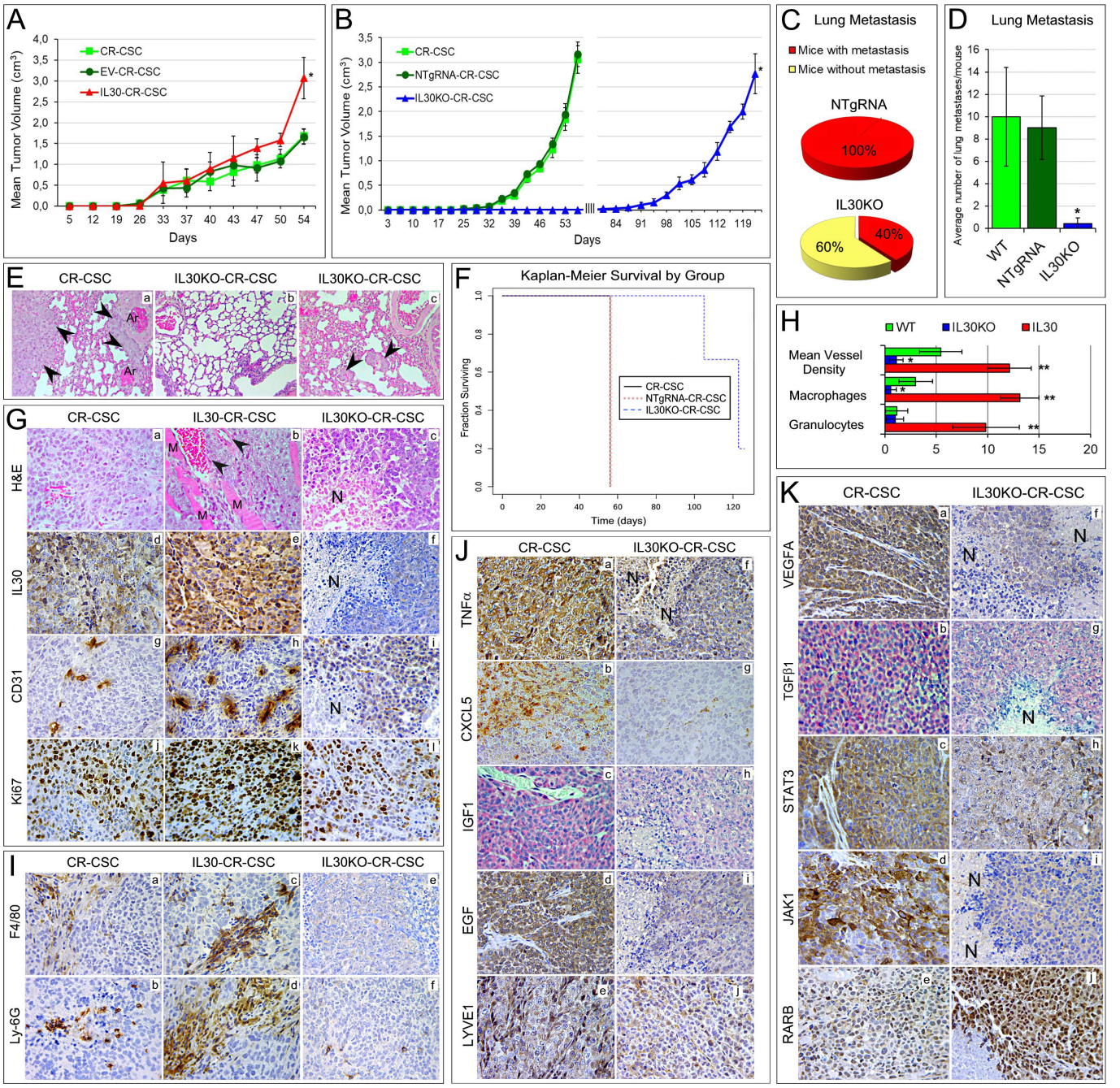

Figure 5 Growth and progression of IL30-deficient or IL30-overexpressing tumors developed after subcutaneous CR-CSC implantation in NSG mice. (A) Mean volume of tumors developed in NSG mice, after s.c. implantation of wild type (WT), EV-CR-CSCs or IL30-CR-CSCs. ANOVA, p<0.0001; *p<0.01 Tukey HSD test versus both CR-CSCs and EV-CR-CSCs. (B) Mean volume of tumors developed in NSG mice, after s.c. implantation of WT, NTgRNA-treated or IL30KO CR-CSCs. ANOVA, p<0.0001; *p<0.01 Tukey HSD test versus both CR-CSCs and NTgRNA-CR-CSCs. (C) Percentages of NSG mice, which spontaneously developed lung metastasis after s.c. injection of WT, NTgRNA-treated or IL30KO CR-CSCs. *Fisher's exact test, p=0.0004 versus NTgRNA or WT tumors. (D) Average number of lung metastasis spontaneously developed in NSG mice bearing tumors induced by WT, NTgRNA-treated or IL30KO CR-CSCs. ANOVA: p<0.0001. *p<0.01, Tukey HSD test compared with WT and NTgRNA tumors. (E) Histopathological features of lungs from tumor bearing NSG mice injected with WT CR-CSCs (a) or IL30KO-CR-CSCs (b, c). Extensive metastatic nodules (arrowheads), developed around small vessels and arterioles (Ar), in mice bearing WT CR-CSC derived tumors. The lungs of 20% of IL30KO tumor-bearing mice were metastases-free (b), while the remaining 80% of mice developed a reduced number of metastases that were usually smaller (arrowheads), compared with the controls. Magnification: ×200. (F) Kaplan-Meier survival curves of mice-bearing tumors developed after s.c. implantation of CR-CSCs, NTgRNA-CR-CSCs or IL30KO-CR-CSCs. Log-rank test: p<0.0001. (G) Immunopathological features of tumors developed in NSG mice after s.c. implantation of WT, IL30 overexpressing or IL30KO CR-CSCs. H&E stained sections showing WT tumor (a) formed by sheets of round to polygonal cancer cells endowed with large nuclei and evident nucleoli. A prominent

Figure 5 continued on next page

Figure 1 continued

vascular supply (arrowheads) and aspects of muscle (M) infiltration are hallmarks of IL30-overexpressing tumor (b), whereas ischemic-hemorrhagic necrosis (N) and loss of cell-to-cell contact characterize IL30KO tumor (c). Expression of IL30 was low, but distinct, in the WT tumor (d), strong in the IL30 gene transfected tumor (e) and absent in the IL30KO tumor (f). The microvessel density was prominent in IL30 gene transfected tumor (h) when compared with the WT tumor (g), whereas it was scanty to absent in the IL30KO tumor (i). The proliferation rate was higher in the IL30 gene transfected tumor (k) than in the WT tumor (j), whereas it was reduced in the IL30KO tumor (l). Results from EV-CR-CSC and NTgRNA-CR-CSC derived tumors were comparable to those obtained from WT tumors (CR-CSC). Magnification: ×400. (H) Automated immune cell count and MVD in tumors developed in NSG mice, after implantation of WT, IL30KO and IL30-CR-CSCs, assessed by immunohistochemistry. ANOVA, p<0.0001. *p<0.01, Tukey HSD test compared with WT tumors. **p<0.01, Tukey HSD test compared with WT and IL30KO tumors. Results obtained from EV and NTgRNA tumors were comparable with those of WT tumors. (I) Immunohistochemical features of the immune cell infiltrate in tumors developed after s.c. implantation of CR-CSCs (a, b), IL30-CR-CSCs (c, d) or IL30KO-CR-CSCs (e, f), show F4/80^{+}macrophages and Ly-6G^{+}granulocytes, which were more represented in IL30-overexpressing tumors (c, d) than in WT control tumors (a, b), but were scarce to absent in IL30 deficient tumors (e, f). Results from EV-CR-CSC and NTgRNA-CR-CSC derived tumors were comparable to those obtained from WT tumors (CR-CSC). Magnification: ×400. F4/80 and Ly-6G stainings in IL30-CR-CSC tumors: X630. (J) Immunohistochemical features of tumors developed in NSG mice after s.c. implantation of WT CR-CSCs (a–e) or IL30KO-CR-CSCs (f–j), show that the expression of TNFα and CXCL5, which was also detected in infiltrating reactive cells, was downregulated in IL30 deficient tumors (f, g) when compared with control tumors (a, b). Expression of both IGF1 and EGF ranged from moderate to strong in WT tumors (c, d), by contrast it was dramatically reduced in IL30KO tumors (h, i). Expression of LYVE1 was marked in tumors induced by WT cells, and localized in both neoplastic cells and lymphatics (e), by contrast it was barely detectable in IL30KO tumors (j). Results from NTgRNA-CR-CSC derived tumors were comparable to those obtained from WT tumors (CR-CSC). N: necrosis. Magnification: X400. (K) Immunohistochemical features of tumors developed in NSG mice after s.c. implantation of WT CR-CSCs (a–e) or IL30KO-CR-CSCs (f–j), show that the expression of VEGFA and TGFβ1 was downregulated in IL30 deficient (IL30KO) tumors (f, g) when compared with WT control tumors (a, b). Expression of STAT3 and JAK1 was downregulated in IL30 deficient (IL30KO) tumors (h, i) when compared with WT control tumors (c, d). The nuclear expression of RARB was weak in cancer cells of WT tumors (e), whereas it was strong in cancer cells forming IL30KO tumors (j). Results from NTgRNA-CR-CSC derived tumors were comparable to those obtained from WT tumors (CR-CSC). N: necrosis. Magnification: ×400. ANOVA, analysis of variance; CR-CSC, colorectal cancer stem cell; EV, empty vector; s.c., subcutaneously.

and assessed its correlation with patient's clinicopathological profiles (table 1).

Immunostaining showed that IL30 was absent in normal colonic tissue, whereas it was expressed in neoplastic tissue and localized in cancer cells and, or, infiltrating leucocytes, mostly monocytes and macrophages, as demonstrated by IL30/CD68 and IL30/CD14 double stainings (figure 6A,a–c). Morphometric analyses revealed that 18/120, 15.00%, of CRC samples showed IL30 positive staining in cancer cells and a strong IL30 expression in infiltrating leucocytes, thus they were defined as IL30$^{+/+}$CRCs (figure 6B,a). In most of the CRC samples, 87/120, 72.50%, IL30 was expressed in both epithelial and immune cell components, but to a markedly different extent, ranging from weakly positive to negative in the neoplastic epithelia, and from distinct to scanty in the immune cell infiltrate, and therefore were defined as IL30$^{+/-}$CRCs (figure 6B,b). The remaining 15/120, 12.50%, of CRC samples showed IL30 negative staining in cancer cells and a scanty IL30 expression in infiltrating leucocytes, that is, lacked IL30 expression in both the epithelial and immune cell compartments, and thus were defined as IL30$^{-/-}$CRCs (figure 6B,c).

Kaplan-Meier survival analysis (figure 6C) revealed that high levels of IL30 production were associated with a shorter overall survival (OS), since patients bearing IL30$^{+/+}$CRCs had a median OS of only 50 months, whereas more than 50% of patients diagnosed with IL30$^{-/-}$CRCs, which showed the best clinical course, or with IL30$^{+/-}$CRCs, were still alive at the time of the last observation (60 months) (log-rank test, p<0.0001). No significant association between IL30 expression and patients' sex and age, TNM staging and molecular CRC subtype was disclosed by the χ^2 or Fisher's exact test (p>0.05) (table 1).

To validate this clinical finding in a larger cohort of patients, RNA-Seq data of tumor samples from the '*CRC TCGA Nature 2012*' collection, which includes 276 CRC cases, were downloaded from the publicly available cBioportal for Cancer Genomics database.

Since the mRNA expression level of IL30 in CRC samples was never below a Z-score=-2, it was defined high (IL30^{High}CRC) when the Z score was ≥2, and moderate (IL30^{Mod}CRC) when the Z-score was <2. After excluding 34 patients due to their incomplete clinicopathological data, of the remaining 242 cases (online supplemental table S3), 230 were classified as patients bearing IL30^{Mod}CRC (Z-score <2 and >−2) and 12 were classified as patients bearing IL30^{High}CRC (Z score ≥2).

Kaplan-Meier survival curves, calculated after the exclusion of cases that also overexpressed EBI3 or CRLF1, Z-score ≥1 (3/12), to exclude the effects due to IL27 or p28/CRLF1 complex, demonstrated that patients bearing IL30^{High}CRCs, 9/239, 4%, had a median OS of 38.90 months, whereas more than 50% of patients bearing IL30^{Mod}CRCs, 230/239, 96%, were still alive at the time of the last observation (60 months) (log-rank test, p=0.0324) (figure 6D). High levels of IL30 expression in CRC samples were associated with a worse clinical outcome, independently of patients' sex and age, or tumor size, stage, and molecular CRC subtype, as assessed by Cramer's V test (V<0.10, p>0.05). The CIBERSORTx algorithm, used to identify leucocyte populations, which account for IL30 production in the CRC microenvironment,

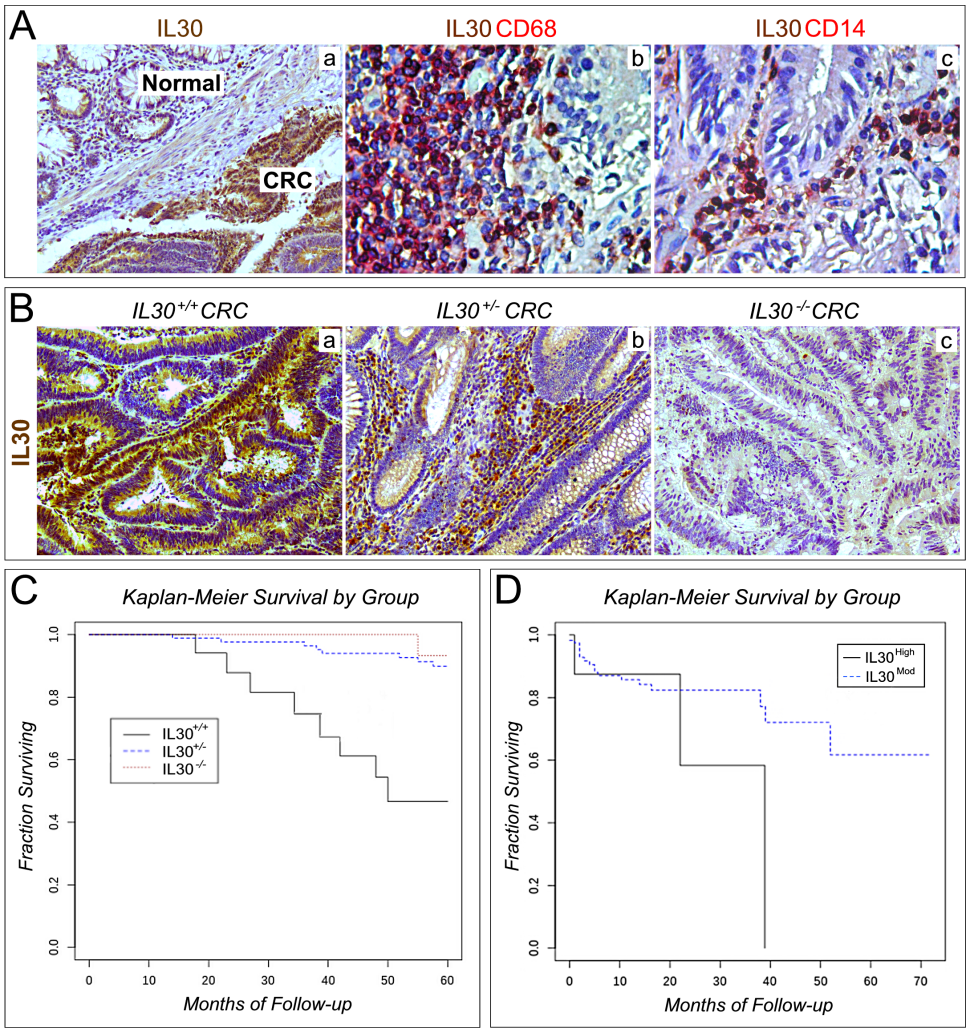

Figure 6 IL30 expression in clinical CRC samples and correlation with patient's overall survival. (A) Immunopathological aspects of CRC and contiguous normal tissue (Normal), showing IL30 expression confined to neoplastic areas (CRC) and involving cancer cells and infiltrating leucocytes (a). Among tumor-infiltrating leucocytes, macrophages and monocytes appeared to be the main source of production of IL30, as shown by IL30/CD68 (b) and IL30/CD14 (c) double stainings. Magnification: ×400. (B) In the CRC tissue samples, IL30 can be strongly expressed in both, epithelial and leucocyte compartments ($IL30^{+/+}$CRC) (a). Otherwise, IL30 can be expressed, to a variable extent, in the neoplastic epithelium, ranging from weakly positive to negative and/or in tumor-infiltrating leucocytes, ranging from distinct to scanty ($IL30^{+/-}$CRC) (b). IL30 expression may be lacked in both epithelial and leucocyte components ($IL30^{-/-}$ CRCs) (c). Magnification: ×400. (C) Kaplan-Meier curves representing, for each time point, the fraction of surviving CRC patients classified, based on IL30 protein expression in tumor cells and infiltrating leucocytes, as patients bearing $IL30^{+/+}$CRCs (n. 18), $IL30^{-/+}$CRCs (n. 87) or $IL30^{-/-}$CRCs (n. 15).(D) Kaplan-Meier curves representing, for each time point, the fraction of surviving CRC patients from the '*Colorectal Adenocarcinoma TCGA Nature 2012*' collection, classified, based on *IL30 mRNA* expression in their clinical samples, as patients bearing $IL30^{High}$CRCs (n. 9) or $IL30^{Mod}$CRCs (n. 230). CRC, colorectal cancer.

revealed that IL30 was mainly expressed by monocytes and macrophages. This data corroborated the immunohistochemical evidence of IL30 production by $CD14^{+}$cells and $CD68^{+}$cells in clinical CRC samples and confirms the contribution of myeloid-derived cells in the production of IL30 in the tumor microenvironment,[9] and therefore, to the regulation of CRC behavior and patient outcome.[4 5 11]

DISCUSSION

The predicted increase in CRC incidence worldwide[1] demands the development of new strategies to prevent and/or treat this deadly malignancy. Since biostatistics revealed that, although to a variable extent, the vast majority of CRCs express IL30, the new data, provided by this study, on its role in CRC tumorigenesis and progression, prompts the development of an IL30 targeting strategy amenable to translation into clinical practice.

CRC onset and progression are driven by a dynamic subset of CSCs,[3] which can shift from slow cycling to actively proliferating, depending on endogenous and microenvironmental signals. Among the regulators of CSC behavior and tumor progression, IL30 has recently proven to be a key player.[4 5 11] Here, we provide evidence

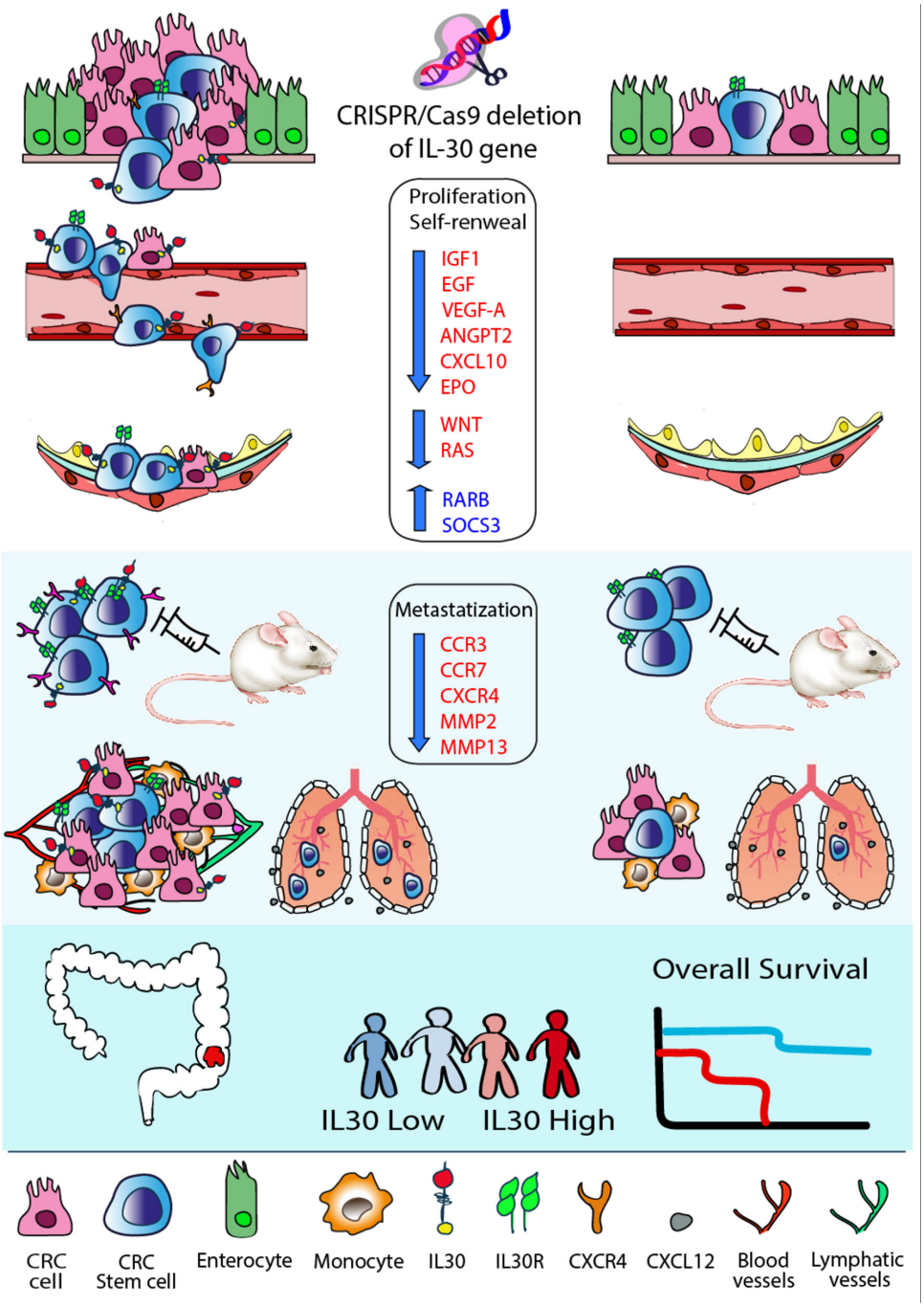

Figure 7 Illustration of the main biological events promoted by IL30 in stem and non-stem CRC cells and in tumor xenografts models of CRC, and representation of the clinical impact of IL30 expression in CRC, based on bioinformatics data and immunopathology studies on tumors from CRC patients. CRISPR/Cas9-mediated deletion of IL30 gene inhibits self-renewal and/or proliferation and migration of stem and non-stem CRC cells, downregulates IGF1, EGF, VEGFA, ANGPT2, CXCL10, EPO, MMP2, MMP13, CCR3, CCR7 and CXCR4, suppresses WNT and RAS family member expression, and upregulates tumor suppressors RARB and SOCS3. Deletion of IL30 gene in CR-CSCs counteracts/delays the onset of the tumor, which has a poor hematic and lymphatic support, low growth and metastatic potential. Kaplan-Meier survival analysis shows that high levels of IL30 expression in CRC tissue specimens are associated with low patient survival. CRC, colorectal cancer; CR-CSCs, colorectal cancer stem cells.

that both stem and differentiated CRC cells constitutively express membrane-anchored IL30, as confirmed by immunogold electron microscopy, and that it regulates genes coding for growth, angiogenic and lymphangiogenic factors, and boosts CSC self-renewal, which involves WNT and RAS family members, such as WNT5A and RAB33A, and expansion of both stem and differentiated CRC cell compartments. In a model of CRC xenograft, IL30 overexpression by CR-CSCs accelerates tumor growth, in association with a significant proliferation,

vascularization and reactive macrophage and granulocyte infiltrate. The tumor progression program triggered by IL30 in both stem and differentiated CRC cells, primarily includes the upregulation of ANGPT2, CXCL10, EPO, IGF1, EGF and VEGFA. While the latter can only act in a paracrine fashion, improving lymphatic and hematic vascular networks,[33] the remaining factors, by binding to their cognate receptors expressed on cancer cells, have proven to feed autocrine growth loops that are amplified and used by IL30 to boost cancer proliferation. IL30-dependent regulation of VEGFA, CXCL10 and EGF has already been found in prostate and breast CSCs,[4 5] while IGF1, EPO and ANGPT2 emerge as new components of the signaling cascade orchestrated by IL30 to support stem and differentiated CRC cell compartments.

Mounting evidence has demonstrated that IGF1-IGF1R signaling is critical for CRC initiation and progression,[35] and that it is associated with metastasis and poor prognosis.[35]

By binding to the EPOR, the hematopoietic cytokine, EPO, promotes survival, proliferation, and differentiation of the early erythropoiesis progenitors, thus supporting erythrocyte production and maturation. However, EPOR expression by endothelial and cancer cells,[36] or by CR-CSCs, as reported in this study, can promote angiogenesis and malignant progression.[36]

By binding to TIE2 on endothelial cells, ANGPT2 promotes vascular remodeling and angiogenesis**,** and cooperates with VEGF to foster tumor development.[37] As for EPO-EPOR signaling, the expression of TIE2, already detected in different CRC cell lines, and here demonstrated in CR-CSCs, implies an autocrine signaling loop mediated by ANGPT2, which fosters IL30-dependent CSC proliferation, thus favoring tumor progression.

In addition to promoting angiogenesis, IL30 regulates in both the stem and non-stem CRC cells, the expression of the lymphatic endothelial cell marker LYVE1, which could favor not only cancer cell migration,[21] but also the 'lymphatic mimicry' whereby cancer cells contribute to the formation of lymphatic vessel walls, ultimately promoting the lymphatic route of metastasis.[33] Metastasization substantially declined because of IL30 deletion in CR-CSCs, since the number of metastatic animals, and the number of metastases per animal, were drastically reduced among IL30 deficient versus WT tumor bearing hosts. Among the molecular mechanisms underlying the anti-metastatic effects of IL30 deletion in CR-CSCs, the significant downmodulation of chemokine receptors, such as CCR3, CCR7 and mostly CXCR4, may be of relevance,[32] as strongly suggested by the inability of IL30KO-CR-CSCs, or anti-IL30 Ab treated WT and IL30 overexpressing CR-CSCs, to migrate in response to CXCL12 due to the suppressed cancer cell expression of its receptor, CXCR4. The molecular mechanism underlying the IL30-dependent regulation of CXCR4 and, therefore, of the migratory potential of CR-CSCs, is revealed by the lack of CXCR4 upregulation in IL30 overexpressing CR-CSCs with the targeted deletion of the *STAT3* gene, which is confirmed as the key signaling molecule in mediating the pro-metastatic effects of IL30.[4 38 39]

Inflammation, a hallmark of cancer, was substantially shut down by IL30 deletion, which, apart from the upregulation of *CCL3,* inhibited the expression of a wide range of chemokines, such as *CCL2, CCL20, CXCL5, CXCL10, CXCL11* and *CXCL17*, and inflammatory or tumor promoting cytokines, such as *IL13, IL32, IL17* and *OSM*.

The imbalance in the regulation of the proteases, MMP and ADAM family members, and protease inhibitors, such as *SERPIN5 and SERPINI2*, with a clear prevalence in the suppression of the former, could also assist in mediating the anti-metastatic effect of IL30-deletion in CR-CSCs.

A significant anti-tumor progression mechanism triggered by IL30 inactivation is the downregulation of genes coding for extracellular matrix proteins, such as *COL24A1, COL5A3, COL9A1, MUC8, MUC15* and *MUC6*, which, by strengthening the ECM meshwork, can promote cancer cell survival and colonization at distant sites.[40]

A role in cancer progression and metastasis formation has also been recognized for *ZNFs,*[41] that are substantially downregulated by IL30 deletion and implicated in a variety of cellular processes, such as transcriptional regulation, ubiquitin-mediated protein degradation, signal transduction, actin targeting, DNA repair and cell migration,[41] although the specific function of each of the ZNFs in colorectal tumorigenesis remains to be investigated.

IL30's ability to shape the immunological profile of neoplastic cells, which has already been demonstrated in prostate and breast tumors,[4 5 11] also occurs in both stem and non-stem CRC cells, in which the inactivation of the IL30 gene downregulates *NOS2*, which is deeply involved in colon carcinogenesis,[30] while it upregulates *GBP1*, which acts as CRC suppressor,[29] along with cell surface molecules, such as *CD96* and *CIITA*. Commonly expressed on T and NK cells, *CD96,* may enhance $CD8^{+}$T cell activation and effector functions, and its expression in cancer may favor immune cell infiltration.[28] *CIITA*-driven MHC Class II expression by cancer cells allows tumor antigen presentation and priming of naïve Th cells, promoting the development of anti-tumor effector responses.

Importantly, IL30 deletion leads to a weakening of the oncogenic pathways closely related to colorectal tumorigenesis, since it dramatically suppresses the expression of WNT and RAS family members, mostly *WNT3, WNT5A, RAB3C* and *RAB33A*, and expression of canonical CRC driver genes, including *TGFB1, TRIB1/2/3 AKT1/3, CRIPTO1, APC2, ALK, MYC, STAT1/3* and *JAK1*. By contrast, the tumor suppressors *SOCS3* and *RARB*, which were lost in CR-CSC-induced WT tumors and re-expressed in IL30-defective tumors, were strongly upregulated because of IL30 gene inactivation.

The clinical value of the in vitro and in vivo experimental findings is strongly suggested by the Kaplan-Meier curves constructed based on bioinformatics of publicly available clinical-pathological data from the '*CRC TCGA Nature 2012*' collection, and immunopathological analyses of CRC samples from a distinct cohort of patients.

The survival curves, together with the survey carried out with the CIBERSORTx analytical tool, reveal that, **i**) IL30 is expressed in most of CRC samples, by cancer cells or infiltrating immune cells, mostly macrophages and monocytes, or both components, and **ii**) the lack of IL30 expression is associated with an increased OS for patients diagnosed with $IL30^{-/-}$CRC, compared with patients with $IL30^{+/-}$CRC or $IL30^{+/+}$CRC. Previous studies have highlighted the driving role of IL30 in tumor onset and progression and the clinical implication of its production in prostate and breast cancer samples.[4 5 11 42 43] IL30 production by tumor cells and leucocytes infiltrating the draining lymph nodes has been found in the majority of metastatic prostate cancers and is tightly linked with advanced disease grade and stage.[42] In breast cancer, IL30 expression mostly involves $HER2^{+}$ and triple-negative tumors. However, independently of the molecular subtype of the tumor, univariate analyses revealed that a high level of IL30 expression by leucocyte infiltrating breast cancer-draining lymph nodes was associated with disease recurrence, and the Cox proportional hazard model, showed a significant association with breast cancer-related mortality.[43] IL30 fueled tumor escape mechanisms, such as the upregulation of PD-L1 and LAG3,[4 5] and T regulatory cell (Treg) recruitment,[5 11] demonstrated in IL30 overexpressing preclinical tumor models and highly suggested by the biostatistical data from patients bearing $IL30^{Positive}$ prostate or breast cancers, could also have important clinical implications. Immune exhaustion with high levels of expression of PD-L1 and LAG-3 correlates with a shorter OS in CRC patients,[44] and accumulation of Tregs has been associated with CRC progression and metastasis, immunotherapy failure and a poorer prognosis.[45]

So far, the role of IL30 in colorectal tumorigenesis has never been explored. Here, we provide evidence that IL30 expressed, as membrane-anchored cytokine, in both stem and non-stem CRC cells, regulates their viability, immunophenotype and tumor progression programs. Targeting of IL30, via CRISPR/Cas9 genome editing, inhibits CR-CSC tumorigenicity and metastatic ability, severely compromises the tumor 'lymphangiogenic switch' and disables oncogenic and proinflammatory pathways, hindering tumor onset and progression (as summarized in the figure 7). This study provides the proof of concept that targeting of IL30 in CR-CSCs inhibits CRC tumorigenesis and envisages its pharmacological development to expand the therapeutic landscape of CRC.

Contributors EDC conceived the study. LD, CF, SLC, SV and LL performed the experiments. LD, CF and CS collected and assembled the data. EDC and CS performed data analyses. EDC interpreted the data, wrote the manuscript and is responsible for the overall content (guarantor). All authors read and approved the final manuscript.

Funding The research leading to these results has received funding from AIRC, under IG 2019-ID. 23264 project—P.I. Di Carlo Emma, and from the Italian Ministry of University and Research (PRIN—2017M8YMR8—Unit 3 P.I. Di Carlo Emma).

Competing interests None declared.

Patient consent for publication Not applicable.

Ethics approval All animal procedures were performed in accordance with the European Community and ARRIVE guidelines and were approved by the Institutional Animal Care Committee of 'G. d'Annunzio' University and by the Italian Ministry of Health (Authorization n. 399/2015 PR). The study was approved by the Ethical Committee of the 'G. d'Annunzio' University and Local Health Authority of Chieti (Reference number: 26/4/12), and was performed, after written informed consent from patients, in accordance with the principles outlined in the Declaration of Helsinki.

Provenance and peer review Not commissioned; externally peer reviewed.

Data availability statement Data are available on reasonable request. The data generated in this study are available on request from the corresponding author. Expression profile data of tumor samples from the '*CRC TCGA Nature 2012*' collection were obtained from the cBioportal for Cancer Genomics database (https://www.cbioportal.org; cBioPortal, RRID:SCR_014555).

ORCID iDs
Cristiano Fieni http://orcid.org/0000-0001-7203-6545
Emma Di Carlo http://orcid.org/0000-0001-7778-1042

REFERENCES

1 Siegel RL, Miller KD, Fuchs HE, *et al*. Cancer statistics, 2022. *CA Cancer J Clin* 2022;72:7–33.
2 Munro MJ, Wickremesekera SK, Peng L, *et al*. Cancer stem cells in colorectal cancer: a review. *J Clin Pathol* 2018;71:110–6.
3 Gupta PB, Pastushenko I, Skibinski A, *et al*. Phenotypic plasticity: driver of cancer initiation, progression, and therapy resistance. *Cell Stem Cell* 2019;24:65–78.
4 Sorrentino C, Ciummo SL, Cipollone G, *et al*. Interleukin-30/il27p28 shapes prostate cancer stem-like cell behavior and is critical for tumor onset and metastasization. *Cancer Res* 2018;78:2654–68.
5 Sorrentino C, Ciummo SL, D'Antonio L, *et al*. Interleukin-30 feeds breast cancer stem cells via CXCL10 and IL23 autocrine loops and shapes immune contexture and host outcome. *J Immunother Cancer* 2021;9:e002966.
6 Pflanz S, Timans JC, Cheung J, *et al*. Il-27, a heterodimeric cytokine composed of EBI3 and p28 protein, induces proliferation of naive CD4+ T cells. *Immunity* 2002;16:779–90.
7 Garbers C, Hermanns HM, Schaper F, *et al*. Plasticity and cross-talk of interleukin 6-type cytokines. *Cytokine Growth Factor Rev* 2012;23:85–97.
8 Liu X, Wang Z, Ye N, *et al*. A protective role of IL-30 via STAT and ERK signaling pathways in macrophage-mediated inflammation. *Biochem Biophys Res Commun* 2013;435:306–12.
9 Di Carlo E. Decoding the role of interleukin-30 in the crosstalk between cancer and myeloid cells. *Cells* 2020;9:615.
10 Garbers C, Spudy B, Aparicio-Siegmund S, *et al*. An interleukin-6 receptor-dependent molecular switch mediates signal transduction of the IL-27 cytokine subunit p28 (IL-30) via a gp130 protein receptor homodimer. *J Biol Chem* 2013;288:4346–54.
11 Sorrentino C, Yin Z, Ciummo S, *et al*. Targeting interleukin(IL)-30/IL-27p28 signaling in cancer stem-like cells and host environment synergistically inhibits prostate cancer growth and improves survival. *J Immunother Cancer* 2019;7:201.
12 Kaushik I, Ramachandran S, Srivastava SK. CRISPR-cas9: a multifaceted therapeutic strategy for cancer treatment. *Semin Cell Dev Biol* 2019;96:4–12.
13 Brattain MG, Fine WD, Khaled FM, *et al*. Heterogeneity of malignant cells from a human colonic carcinoma. *Cancer Res* 1981;41:1751–6.

14 Müller SI, Friedl A, Aschenbrenner I, *et al*. A folding switch regulates interleukin 27 biogenesis and secretion of its α-subunit as a cytokine. *Proc Natl Acad Sci U S A* 2019;116:1585–90.
15 Jing Y, Jia D, Wong C-M, *et al*. SERPINA5 inhibits tumor cell migration by modulating the fibronectin-integrin β1 signaling pathway in hepatocellular carcinoma. *Mol Oncol* 2014;8:366–77.
16 Loftus SK, Cannons JL, Incao A, *et al*. Acinar cell apoptosis in serpini2-deficient mice models pancreatic insufficiency. *PLoS Genet* 2005;1:e38.
17 Inoue H, Shiraki K, Yamanaka T, *et al*. Functional expression of tumor necrosis factor-related apoptosis-inducing ligand in human colonic adenocarcinoma cells. *Lab Invest* 2002;82:1111–9.
18 Miyoshi H, Ajima R, Luo CT, *et al*. Wnt5A potentiates TGF-β signaling to promote colonic crypt regeneration after tissue injury. *Science* 2012;338:108–13.
19 Moon B-S, Jeong W-J, Park J, *et al*. Role of oncogenic K-Ras in cancer stem cell activation by aberrant Wnt/β-catenin signaling. *J Natl Cancer Inst* 2014;106:djt373.
20 Modarai SR, Gupta A, Opdenaker LM, *et al*. The anti-cancer effect of retinoic acid signaling in CRC occurs via decreased growth of ALDH+ colon cancer stem cells and increased differentiation of stem cells. *Oncotarget* 2018;9:34658–69.
21 Jackson DG, Prevo R, Clasper S, *et al*. Lyve-1, the lymphatic system and tumor lymphangiogenesis. *Trends Immunol* 2001;22:317–21.
22 Berx G, van Roy F. Involvement of members of the cadherin superfamily in cancer. *Cold Spring Harb Perspect Biol* 2009;1:a003129.
23 Maione F, Molla F, Meda C, *et al*. Semaphorin 3A is an endogenous angiogenesis inhibitor that blocks tumor growth and normalizes tumor vasculature in transgenic mouse models. *J Clin Invest* 2009;119:3356–72.
24 Catalano A, Caprari P, Moretti S, *et al*. Semaphorin-3A is expressed by tumor cells and alters T-cell signal transduction and function. *Blood* 2006;107:3321–9.
25 Lu Y, Xu Q, Chen L, *et al*. Expression of semaphorin 6D and its receptor plexin-A1 in gastric cancer and their association with tumor angiogenesis. *Oncol Lett* 2016;12:3967–74.
26 Dong X, Wang J, Tang B, *et al*. The role and gene expression profile of SOCS3 in colorectal carcinoma. *Oncotarget* 2018;9:15984–96.
27 Tobelaim WS, Beaurivage C, Champagne A, *et al*. Tumour-promoting role of SOCS1 in colorectal cancer cells. *Sci Rep* 2015;5:14301.
28 Mittal D, Lepletier A, Madore J, *et al*. Cd96 is an immune checkpoint that regulates CD8+ T-cell antitumor function. *Cancer Immunol Res* 2019;7:559–71.
29 Britzen-Laurent N, Lipnik K, Ocker M, *et al*. GBP-1 acts as a tumor suppressor in colorectal cancer cells. *Carcinogenesis* 2013;34:153–62.
30 de Oliveira GA, Cheng RYS, Ridnour LA, *et al*. Inducible nitric oxide synthase in the carcinogenesis of gastrointestinal cancers. *Antioxid Redox Signal* 2017;26:1059–77.
31 Mollica Poeta V, Massara M, Capucetti A, *et al*. Chemokines and chemokine receptors: new targets for cancer immunotherapy. *Front Immunol* 2019;10:379.
32 Céspedes MV, Unzueta U, Aviñó A, *et al*. Selective depletion of metastatic stem cells as therapy for human colorectal cancer. *EMBO Mol Med* 2018;10.
33 Karinen S, Juurikka K, Hujanen R, *et al*. Tumour cells express functional lymphatic endothelium-specific hyaluronan receptor in vitro and in vivo: lymphatic mimicry promotes oral oncogenesis? *Oncogenesis* 2021;10:23.
34 Hanrahan V, Currie MJ, Gunningham SP, *et al*. The angiogenic switch for vascular endothelial growth factor (VEGF)-A, VEGF-B, VEGF-C, and VEGF-D in the adenoma-carcinoma sequence during colorectal cancer progression. *J Pathol* 2003;200:183–94.
35 Murphy N, Carreras-Torres R, Song M, *et al*. Circulating levels of insulin-like growth factor 1 and insulin-like growth factor binding protein 3 associate with risk of colorectal cancer based on serologic and mendelian randomization analyses. *Gastroenterology* 2020;158:1300–12.
36 Hardee ME, Arcasoy MO, Blackwell KL, *et al*. Erythropoietin biology in cancer. *Clin Cancer Res* 2006;12:332–9.
37 Yoshiji H, Kuriyama S, Noguchi R, *et al*. Angiopoietin 2 displays a vascular endothelial growth factor dependent synergistic effect in hepatocellular carcinoma development in mice. *Gut* 2005;54:1768–75.
38 El-Tanani M, Al Khatib AO, Aladwan SM, *et al*. Importance of STAT3 signalling in cancer, metastasis and therapeutic interventions. *Cell Signal* 2022;92:110275.
39 Lim RZL, Li L, Yong EL, *et al*. STAT-3 regulation of CXCR4 is necessary for the prenylflavonoid icaritin to enhance mesenchymal stem cell proliferation, migration and osteogenic differentiation. *Biochim Biophys Acta Gen Subj* 2018;1862:1680–92.
40 Winkler J, Abisoye-Ogunniyan A, Metcalf KJ, *et al*. Concepts of extracellular matrix remodelling in tumour progression and metastasis. *Nat Commun* 2020;11:5120.
41 Cassandri M, Smirnov A, Novelli F, *et al*. Zinc-finger proteins in health and disease. *Cell Death Discov* 2017;3:17071.
42 Di Meo S, Airoldi I, Sorrentino C, *et al*. Interleukin-30 expression in prostate cancer and its draining lymph nodes correlates with advanced grade and stage. *Clin Cancer Res* 2014;20:585–94.
43 Airoldi I, Cocco C, Sorrentino C, *et al*. Interleukin-30 promotes breast cancer growth and progression. *Cancer Res* 2016;76:6218–29.
44 Sorrentino C, D'Antonio L, Fieni C, *et al*. Colorectal cancer-associated immune exhaustion involves T and B lymphocytes and conventional NK cells and correlates with a shorter overall survival. *Front Immunol* 2021;12:778329.
45 Aristin Revilla S, Kranenburg O, Coffer PJ. Colorectal cancer-infiltrating regulatory T cells: functional heterogeneity, metabolic adaptation, and therapeutic targeting. *Front Immunol* 2022;13:903564.